Experimental Eye Research 191 (2020) 107919

Contents lists available at ScienceDirect

Experimental Eye Research

journal homepage: www.elsevier.com/locate/yexer

Quantitative analysis of metabolites in glucose metabolism in the aqueous humor of patients with central retinal vein occlusion

Pinghui Wei[a,b], Meiqin He[a], He Teng[c], Guoge Han[b,*]

[a] Clinical College of Ophthalmology, Tianjin Medical University, Tianjin, PR China
[b] Tianjin Eye Hospital, Tianjin Eye Institute, Tianjin Key Lab of Ophthalmology and Visual Science, Nankai University, Tianjin, PR China
[c] Eye Institute and School of Optometry and Ophthalmology, Tianjin Medical University Eye Hospital, Tianjin, PR China

ARTICLE INFO

Keywords:
Glucose metabolism
Aqueous humor (AH)
Central retinal vein occlusion (CRVO)
Retinal metabolism

ABSTRACT

Quantitative analysis of aqueous humor (AH) was performed to investigate glucose metabolism in patients with central retinal vein occlusion (CRVO), and to explore metabolic changes after anti-vascular endothelial growth factor (VEGF) treatment. AH samples were collected from 35 patients. Participants diagnosed with CRVO (n = 15) were compared to participants who underwent cataract surgery (n = 20). Thirteen of the participants with CRVO received second-round anti-VEGF treatments. Ultra-high performance liquid chromatography tandem-mass spectrometry (UHPLC-MS/MS) was used to quantify metabolites of the AH. Central macular thickness (CMT) and retinal ganglion cell layer (RGC) thickness were measured using spectral-domain optical coherence tomography. Thirteen metabolites involved in glucose metabolism were identified. Among these metabolites, succinate, glutamate, and glutamine were significantly decreased for the CRVO group ($p = 0.028$, 0.009, and 0.017, respectively). The α-ketoglutarate/citrate (K/C) ratio had a significant positive correlation with glutamine levels for both control ($r = 0.922$, $p < 0.001$) and CRVO groups ($r = 0.674$, $p = 0.006$). A significant increase in lactate was observed after intravitreal anti-VEGF administration ($t = 2.273$, $p = 0.045$); the change in CMT was negatively correlated with this increase ($r = -0.745$, $p = 0.003$). The alteration of RGC thickness was negatively correlated with increases in both glutamine ($r = -0.619$, $p = 0.024$) and glucose ($r = -0.754$, $p = 0.003$). These results indicate that, compared to glucose metabolism, glutamine was significantly decreased in the AH of patients with CRVO, and may therefore serve as a potential target for CRVO therapy. The glycolytic pathway might be enhanced after intravitreal anti-VEGF injection, which is an important insight into CRVO pathophysiology.

1. Introduction

The global prevalence of central retinal vein occlusion (CRVO) is 4.67 million, with a pooled ten-year cumulative incidence rate of 1.63% (Song et al., 2019). The human retina is one of the highest energy-consuming and metabolically active tissues; it is assumed that glucose is essential for its visual function as well as for maintenance of homeostasis (Joyal et al., 2018). Unlike brain tissue, the retinal tissues preferentially produce the majority of their energy via aerobic glycolysis (the Warburg effect), whereby glucose is preferably converted to lactate rather than metabolized via the tricarboxylic acid (TCA) cycle (Winkler, 1981; Winkler et al., 2000, 2004). Under hypoxic conditions, the retinae produce their ATP via upregulation of anaerobic glycolysis, a manifestation of the Pasteur effect (Winkler et al., 2003). For eyes with CRVO, mean oxyhemoglobin saturation is markedly lower than that of unaffected eyes (Eliasdottir, 2018). Oxygen deficiency is often associated with disruptions in metabolic activity, which can deplete ATP stores and impair its generation via glucose metabolism (Eliasdottir, 2018). Although glucose are pivotal for metabolism in the retina (Joyal et al., 2018), limited research elucidated glucose metabolic dysfunction in the presence of ischemia and hypoxia in human eye tissues from CRVO patients.

Glutamine is also an important source of carbon in the tricarboxylic acid (TCA) cycle, where it can either be metabolized in the oxidative or reductive direction. Cells under hypoxia mostly rely on the reductive carboxylation of glutamine-derived α-ketoglutarate (Metallo et al., 2011). A previous study identified the α-ketoglutarate/citrate ratio as a critical determinant of reductive glutamine utilization (Fendt et al., 2013). In the eye tissue, RPE displays a strong capacity for reductive carboxylation, which requires high levels of α-ketoglutarate as a

* Corresponding author. Tianjin Eye Hospital, Tianjin Key Lab of Ophthalmology and Visual Science, Nankai University, No. 4, Gansu Road, Tianjin, 300020, PR China.
E-mail address: dovehanguoge@hotmail.com (G. Han).

https://doi.org/10.1016/j.exer.2020.107919
Received 13 September 2019; Received in revised form 18 December 2019; Accepted 4 January 2020
Available online 08 January 2020
0014-4835/

substrate (Du et al., 2016). Therefore, measuring the ratio of α-ketoglutarate/citrate is important to analyze the cause of metabolite changes in patients with CRVO.

The analysis of total retinal metabolites from diseased human retinas poses some major challenges. In addition to the inaccessibility of retinae tissue specimens, surgical harvesting of vitreous fluid is associated with a risk of vitreous hemorrhage, retinal tears, and retinal detachment (Yao et al., 2013). Alternatively, obtaining aqueous humor (AH) samples is a much simpler and less risky procedure. The AH provides nutrients and metabolic signatures from ocular tissues. Composition of AH depends not only on the nature of its production, but also on metabolic exchanges that occur throughout its intraocular route (Barbas-Bernardos et al., 2016). Metabolites studies are considered more representative of the true functional states of disease phenotypes, since they involve the measurement of changes that occur downstream to those that can be measured using genomics, transcriptomics, and proteomics. The majority of endogenous metabolites are directly involved in the development of disease and measuring their fluctuations can reveal biologically relevant changes within systems at specific stages of disease progression (Trivedi et al., 2017).

The AH metabolomic composition has previously been studied using metabolomics approaches in glaucoma (Mayordomo-Febrer et al., 2015), diabetic retinopathy (DR) (Jin et al., 2019; Wang et al., 2019), and myopia (Barbas-Bernardos et al., 2016; Ji et al., 2017). These studies showed that the metabolite changes in the AH can reflect on the current phenotype of particular ocular diseases. This is also been implemented to help understand pathophysiological processes responsible for disease occurrence and progression. Based on the above examples, we hypothesized that the disruption of AH glucose metabolism homeostasis might play a major role in the development of CRVO. Tandem mass spectrometry coupled with ultrahigh performance liquid chromatography (UHPLC-MS/MS) enables fast and sensitive analyses of small molecules in complex biological systems (Santos-Fandila et al., 2013; Tang et al., 2016). We therefore aimed to utilize UHPLC-MS/MS for the metabolic profiling of AH taken from patients with CRVO. To the best of our knowledge, this is the first paper to quantify alterations in glucose metabolism of the AH from patients with CRVO using UHPLC-MS/MS.

2. Materials and methods

2.1. Participants

This prospective cohort study was performed at Tianjin Eye Hospital. The study protocol was approved by the Tianjin Eye Hospital Ethics Committee, adhered to the tenets of the Declaration of Helsinki and is registered online with the Chinese Clinical Trial Registry (ChiCTR1900022442). All subjects enrolled in the study provided written informed consent.

Participants in this study included 15 patients (15 eyes) with CRVO, who were treated intravitreally with 0.5 mg of ranibizumab between January 2019 and June 2019. The criterion for intravitreal ranibizumab injection therapy was a central macular thickness (CMT) > 300 μm. Thirteen patients underwent a second round of anti-VEGF injections 1 month after the initial treatment, and these comprised the Post-CRVO group. A separate control group included 20 age- and sex-matched undergoing cataract surgery.

All participants underwent a comprehensive eye examination, including the measurement of uncorrected and corrected distance visual acuity, subjective refraction, noncontact tonometry, slit-lamp examination, dilated fundus examination, spectral domain optical coherence tomography (SD-OCT), fluorescein angiography (FA), and indocyanine green angiography (ICGA). Central macular thickness (CMT) and retinal ganglion cell layer (RGC) thickness were measured using SD-OCT.

The exclusion criteria included: the presence of any retinopathy other than CRVO, uveitis or ocular infection, glaucoma, corneal disease, significant media opacities, a spherical equivalent refractive error of 6 diopters or more, past history of retinal surgery, history of any other ocular surgery or intraocular procedure (such as laser and intraocular injections), and diabetes mellitus, with or without concomitant DR.

Table 1
Study population characteristics of the participants in this study (mean ± SD).

Characteristic	Controls(n = 20)	CRVO(n = 15)	p Value
Age, y	69.58 ± 6.75	64.73 ± 3.16	0.128
Female, %	35	46.7	0.486
Alcohol, %	5	6.7	0.833
Smokers, %	5	6.7	0.833
Hypertension, %	40	46.7	0.693
Hyperlipidemia, %	10	20	0.403
Cerebral infarction, %	5	6.7	0.833
Coronary heart disease, %	10	13.3	0.759

Clinical characteristics were compared between CRVO patients and controls using independent *t*-test for continuous variables and a $\chi 2$ test for categorical variables.

2.2. Sample collection

All AH samples were collected before intravitreal injection and cataract surgery in the operating room using an operating microscope. Undiluted samples were transferred into sterile containers and clarified by centrifugation in sterile tubes at 15,000 rpm for 5 min before immediate storage at −80 °C until UHPLC-MS analysis.

2.3. UHPLC-MS analysis

To compensate for the matrix effects of the aqueous humor, the calibration standards were diluted in normal saline solution (0.9% sodium chloride) and prepared in the same way as the samples. Frozen AH samples were thawed and subjected to UHPLC-MS. The metabolite profiling of all samples was conducted as previously reported(Yuan et al., 2012). The LC/MS portion of the platform was based on a Thermo Fisher Vanquish UHPLC equipped with an ACQUITY UPLC BEH Amide column (1.7 μm, 2.1 mm × 100 mm, Waters) and Thermo-TSQ Vantage™ mass spectrometer. Metabolites were detected in electro spray negative-ionization and positive-ionization mode. The ACQUITY UPLC BEH Amide column was heated to 45 °C under a flow rate of 300 μL/min. A gradient was used to separate the compounds consisting of 20 mM ammonium acetate and 5% acetonitrile with PH 9.45(solvent A) and 100% acetonitrile (solvent B). The gradient started at 5% solvent A for 1 min, increased linearly to 35% solvent A over 13 min, and then increased linearly to 60% solvent A over 2 min with a 2 min hold before returning the starting mixture for 0.1 min and re-equilibrating for 4 min. QC samples were injected every six or eight samples during acquisition.

MS conditions were as follows: collision gas pressure (mTorr): 1.0; Q1 peak width (FWHM): 0.70; Q3 peak width (FWHM): 0.70; cycle time (s): 1.500; capillary temperature: 350.0 °C; vaporizer temperature: 350.0 °C; sheath gas pressure: 35.0; aux valve flow: 10.0; spray voltage: positive polarity −3500.0 V; negative polarity −3000.0 V; scan type: selected reaction monitoring/multiple reaction monitoring (SRM/MRM). Standard dilution including 13 metabolites was prepared for LC-MS analysis. The peak area of each standard metabolite was prepared from serially diluted reference standard solutions with the corresponding concentration. Calibration curves were constructed with the least-squares method.

To ensure data quality for metabolic profiling, quality control (QC) samples were prepared by pooling aliquots representative of all samples under analysis and used for data normalization. QC samples were prepared and analyzed with the same procedure as that for

Table 2
Parameters evaluated for performance assessment of UHPLC-MS/MS in this study.

Component Name	MS Mode	RT (min)	Standard Calibration Curve	R^2
Glucose	Neg	8.4	y = 1414.45 + 4.38797*x	0.9994
Phosphoenolpyruvate	Neg	12.7	y = 10953.3*x	0.9984
Pyruvate	Neg	1.8	y = 1500.67*x	0.9621
Lactate	Neg	5.3	y = 31764.1*x	0.9996
Citrate	Neg	12.8	y = 1944.06*x	0.9233
Aconitate	Neg	12.7	y = 8392.7*x	0.9517
Isocitrate	Neg	12.6	y = 26922*x	0.9463
α-Ketoglutarate	Neg	10.5	y = 3223.92*x	0.9993
Succinate	Neg	10.7	y = 46529.6*x	0.9993
Fumarate	Neg	11.1	y = 23618.7*x	0.9988
Malate	Neg	11.1	y = 262827*x	0.9974
Glutamate	Pos	11	y = 221916*x	0.9998
Glutamine	Pos	10.5	y = 493163*x	0.9912

RT: retention time, Neg: negative mode, Pos: positive mode.

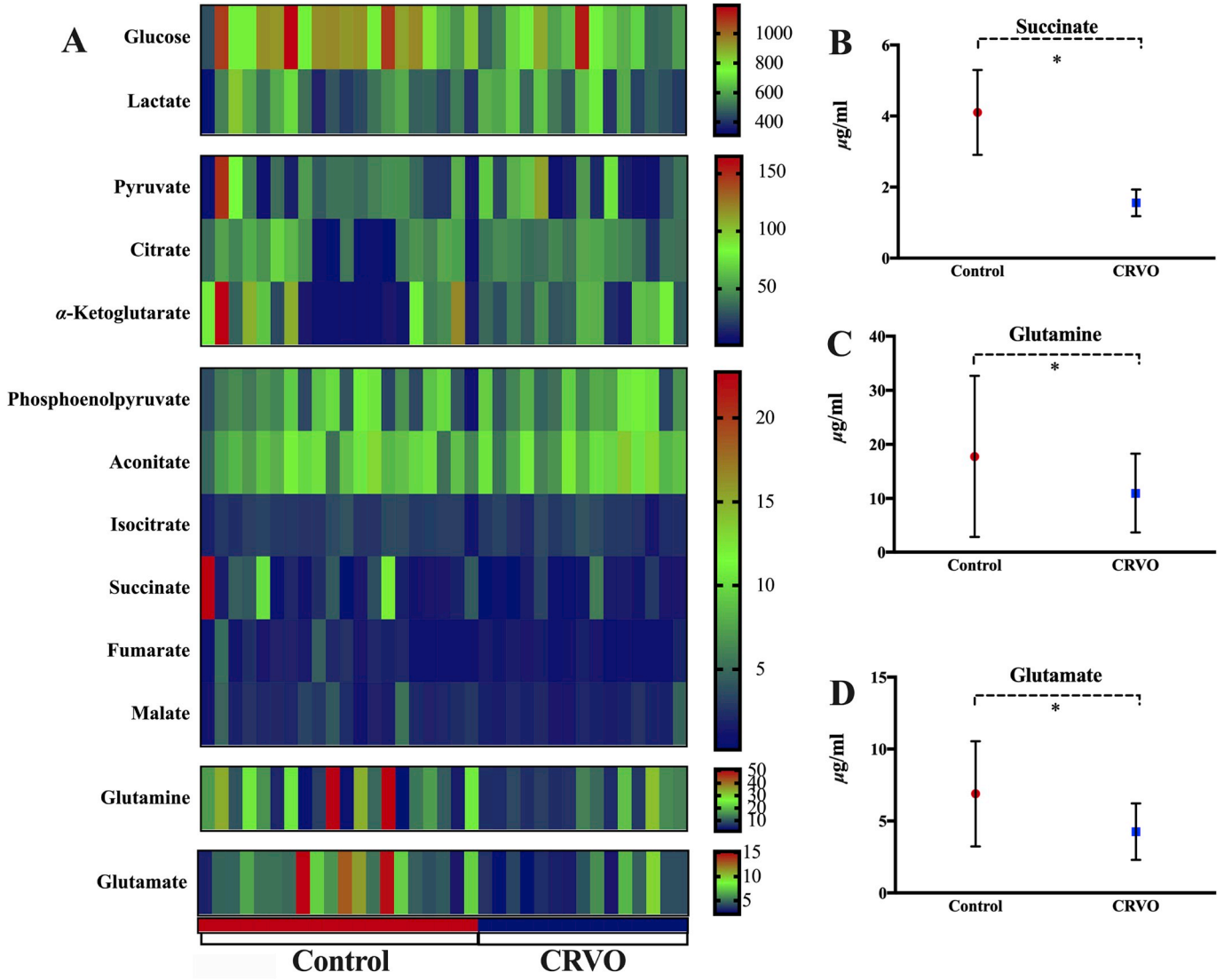

Fig. 1. Concentration of the metabolites quantified by UHPLC-MS/MS between the control and CRVO group. A: Heat map representation of metabolites across 35 samples. Each line in the heat map represented a metabolite. The deeper the red color, the higher its content in the tested sample; similarly, the deeper the blue color, the lower its content in the tested sample; B: The mean succinate level of AH was significantly decreased in the CRVO group when compared to the control group ($p < 0.05$); C: The mean glutamine level of AH was significantly decreased in the CRVO group when compared to the control group ($p < 0.05$). D: The mean glutamate level of AH was significantly decreased in the CRVO group when compared to the control group ($p < 0.05$). (For interpretation of the references to color in this figure legend, the reader is referred to the Web version of this article.)

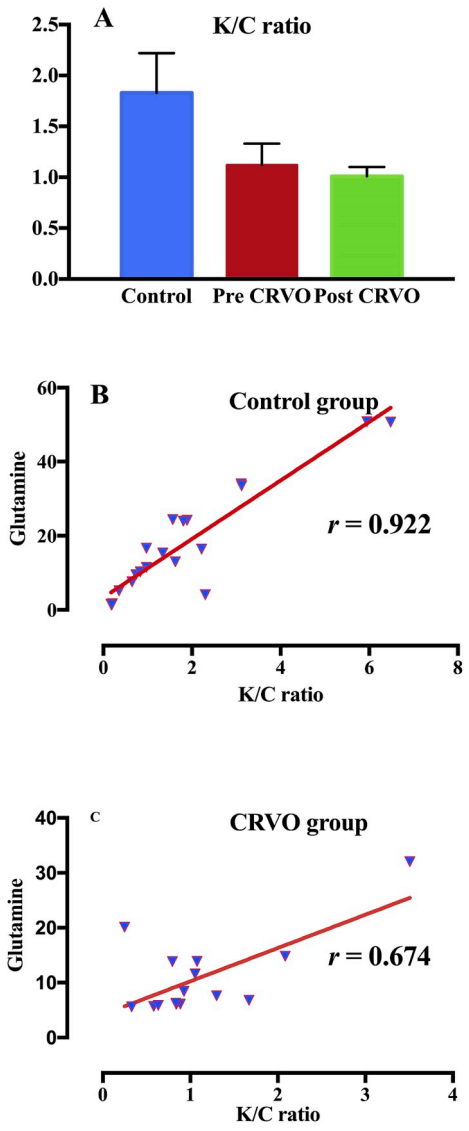

Fig. 2. A: Bar chart showed that the α-ketoglutarate to citrate (K/C) ratio of the CRVO group was lower than that of the control group; B and C: Pearson's correlation coefficients (Pearson r) were computed to investigate the relationship between the K/C ratio and glutamine in the control group and CRVO group.

experimental samples in each batch. Metabolites with QC-RSD (relative standard deviation) less than 30% were regarded as accepted data QC in terms of stability and reliability (Fig. S1). Dried extracts were dissolved in 50% acetonitrile. Each sample was filtered with a disposable 0.22 μm cellulose acetate membrane, transferred into 2 mL HPLC vials, and stored at −80 °C until analysis. Succinate-d6 (CIL, Cambridge Isotope Laboratories) was spiked in every sample before metabolite extraction, and used as internal standards with transitions 122 → 102 and 122 → 78. The Standard LC-MS XIC are shown in Fig. S2.

2.4. Data preprocessing and filtering

Raw SRM data files were processed by peak finding, alignment, and filtering using Xcalibur Qual browser software. The concentration of each metabolite was calculated from the calibration curve of corresponding standard metabolites.

2.5. Statistical analysis

Statistical analysis was performed using SPSS software v21 (IBM Corp., Armonk, NY, USA). All data were tested with the Kolmogorov-Smirnov test and were normally distributed. Differences in metabolite levels were compared between patients with CRVO before intravitreal anti-VEGF injections and controls using independent Student's t-test and expressed as mean ± standard deviation (SD). A paired *t*-test was used to compare differences in metabolite levels before and after intravitreal anti-VEGF injections. Pearson's correlation coefficients were computed to investigate linear relationships between variables. P-values less than 0.05 were considered statistically significant.

3. Results

3.1. Clinical characteristics of participants

The study population consisted of 35 patients, including 15 patients with CRVO and 20 cataracts. There were no differences in demographic variables or comorbidities between the CRVO and control groups (Table 1).

3.2. Metabolic variation between patients with CRVO and controls

A total of 13 metabolites related to carbohydrate metabolism signaling pathways, including 4 glycolysis metabolites, 7 tricarboxylic acid (TCA) cycle intermediates, and glutamine/glutamate were detected in our study (Table 2). A comparison between the metabolite levels for patients with CRVO and controls is presented in Fig. 1. As shown in Fig. 1A, three identified metabolites displayed remarkable diversity in their abundances across the 35 tested samples. Of these metabolites, succinate exhibited the most significant decrease ($t = -2.200$, $p = 0.028$; Fig. 1B). In terms of glutamate and glutamine, the AH of controls had concentrations of 6.89 ± 3.65 and 18.35 ± 14.94 μg/ml, respectively; whereas the corresponding values in the CRVO group were significantly lower at 4.26 ± 1.96 μg/ml ($t = 3.053$, $p = 0.009$) and 10.96 ± 7.30 μg/ml ($t = 2.525$, $p = 0.017$), respectively(Fig. 1C–D). No other metabolites differed significantly between the two groups.

3.3. Changes in human AH α-ketoglutarate to citrate (K/C) ratios

Using UHPLC-MS/MS, we quantitatively assessed K/C ratios in the AH. Although no statistical differences were detected, the K/C ratio of eyes with CRVO was decreased compared to cataract controls (Fig. 2A). Correlation analysis of K/C values revealed a highly significant correlation between K/C ratio and glutamine levels for both the control ($r = 0.922$, $p < 0.001$, Fig. 2B) and CRVO ($r = 0.674$, $p = 0.006$, Fig. 2C) groups.

3.4. Metabolic changes in human AH after intravitreal anti-VEGF injection

As shown in Fig. 3, almost all metabolites exhibited an upward trend after intravitreal anti-VEGF injection. Among them, lactate was significantly increased ($t = 2.273$, $p = 0.045$; Fig. 3C); however, no significant changes were detected for other metabolites.

3.5. Negative correlation of metabolic changes in AH of CRVO with CMT and RGC thickness alteration after intravitreal anti-VEGF injection

Changes in central macular thickness (CMT) were negatively correlated with changes in glucose ($r = -0.704$, $p = 0.007$; Fig. 4A) and lactate ($r = -0.745$, $p = 0.003$; Fig. 4B). Changes in the retinal ganglion cell layer (RGC) after intravitreal anti-VEGF injection were negatively correlated with changes in glucose ($r = -0.754$, $p = 0.003$; Fig. 4C) and glutamine ($r = -0.619$, $p = 0.024$; Fig. 4D).

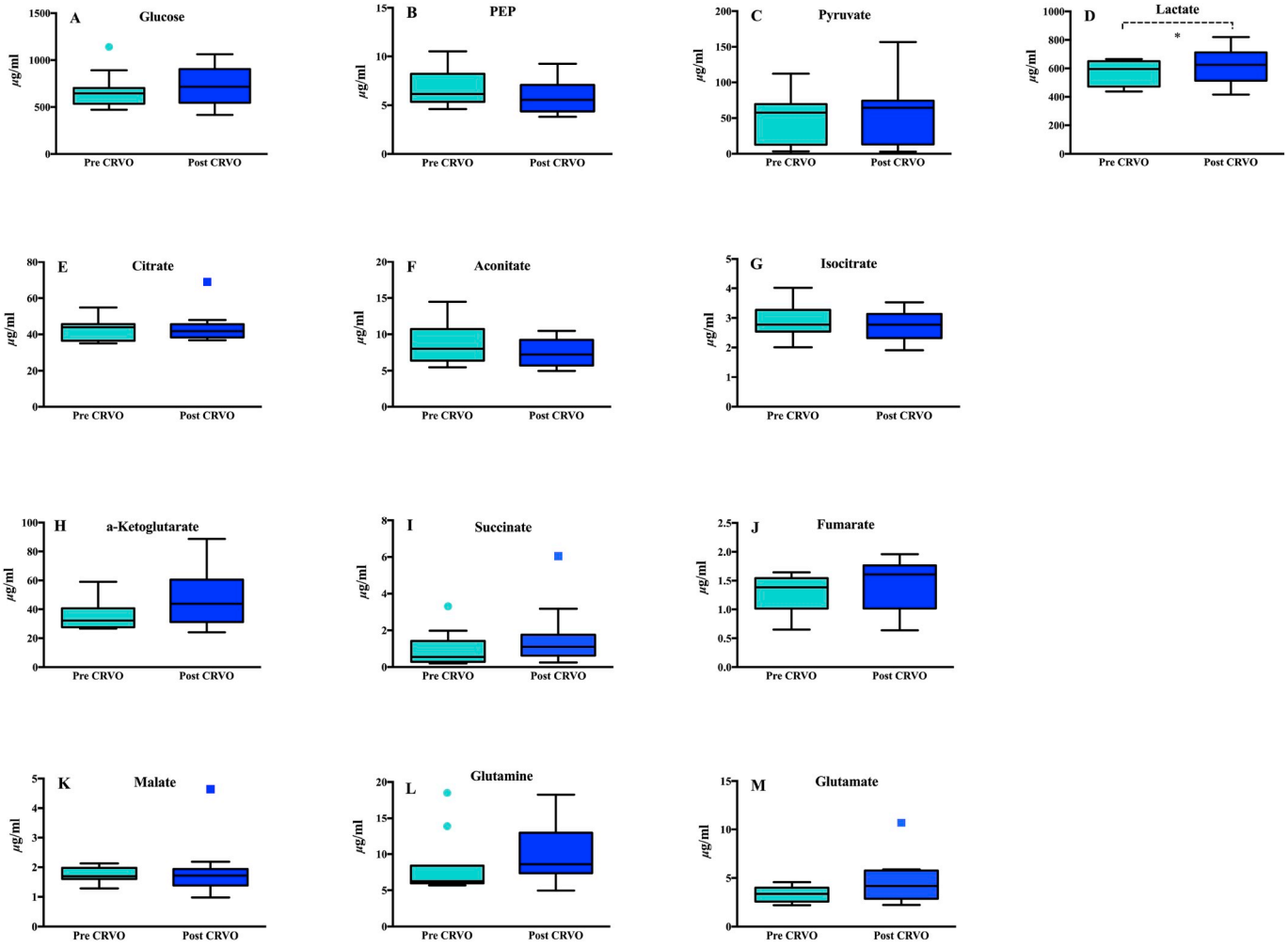

Fig. 3. Concentration of the glucose metabolism related molecules in AH quantified by UPLC-MS/MS between Pre-CRVO and Post-CRVO groups. Thirteen metabolites related to glucose metabolism were identified and absolute quantified in AH analyzed samples. The paired *t*-test results of detected metabolites in human AH after intravitreal anti-VEGF injection are summarized in the box plots; Pre-CRVO: patients with CRVO before intravitreal anti-VEGF injection; Post-CRVO: patients with CRVO after intravitreal anti-VEGF injection; * statistically significant ($p < 0.05$).

4. Discussion

In CRVO, the outflow of the central retinal vein is impaired, which can further disrupt metabolic activities of the retina. Quantitative metabolomics is becoming an increasingly important tool for identifying the pathophysiological mechanisms and biomarkers of diseases at the molecular level. Among the analytical platforms used in metabolomics, liquid chromatography-mass spectrometry (LC-MS) allows for the highest metabolome coverage (Lains et al., 2019; Young and Wallace, 2009). In the present study, UHPLC-MS/MS was used to quantify variations in AH metabolites between patients with CRVO and controls. The AH provides metabolic exchange with surrounding tissues throughout its intraocular route; therefore, the application of UHPLC-MS/MS to study human AH may provide new knowledge concerning the molecular mechanisms behind the pathogenesis of CRVO. In addition, understanding metabolic adaptations to low blood flow may be informative for the treatment of ischemic retinopathy.

Our analyses included a total of 13 metabolites related to metabolic signaling pathways, of which lactate and glucose were the most concentrated, followed by pyruvate and citrate (Fig. 2A). These findings are in agreement with the previously reported metabolomic profile for the AH from cataract patients (Snytnikova et al., 2016). Thus, comparative analyses of AH metabolite studies using UHPLC-MS/MS may provide important information regarding metabolic processes taking place in human CRVO eye tissues.

Glutamate and glutamine levels were significantly lower in the CRVO group compared to controls (Fig. 2B and C). A previous study (Rhee et al., 2018) found that plasma glutamine and glutamate are decreased in DR and therefore suggested that these metabolites may be valuable biomarkers of DR. Other studies have also found that decreased glutamine levels in the vitreous fluid of patients with DR (Ishikawa et al., 1995) and the AH of patients with retinal artery occlusion (Hu et al., 2012; Hurley et al., 2015). There are several possible explanations for decreased glutamine levels in AH. In CRVO, the outflow of the central retinal vein is impaired, which could disrupt metabolic activities and hence inhibit the synthesis of glutamine. Glutamine is synthesized by the enzyme glutamine synthetase (GS) (Joyal et al., 2018), a process that consumes ATP. In the presence of ischemic injury, GS expression is perturbed, leading to a reduction in glutamine within ciliary nonpigmented epithelial cells (NPE) and thus a reduction in its efflux into the AH (Hu et al., 2012). Moreover, glutamine was utilized to be converted to precursors of gluconeogenesis (Wu, 2009), the decreased glutamine levels could be due to the increased catabolism for energy production under retinal ischemia condition (Drake et al., 2012; Trainor et al., 2017).

In standard growth conditions, proliferation-relevant fatty acids are barely produced from glutamine (Fendt et al., 2013). During hypoxia or mitochondrial inhibition, glutamine conversion from oxidative to

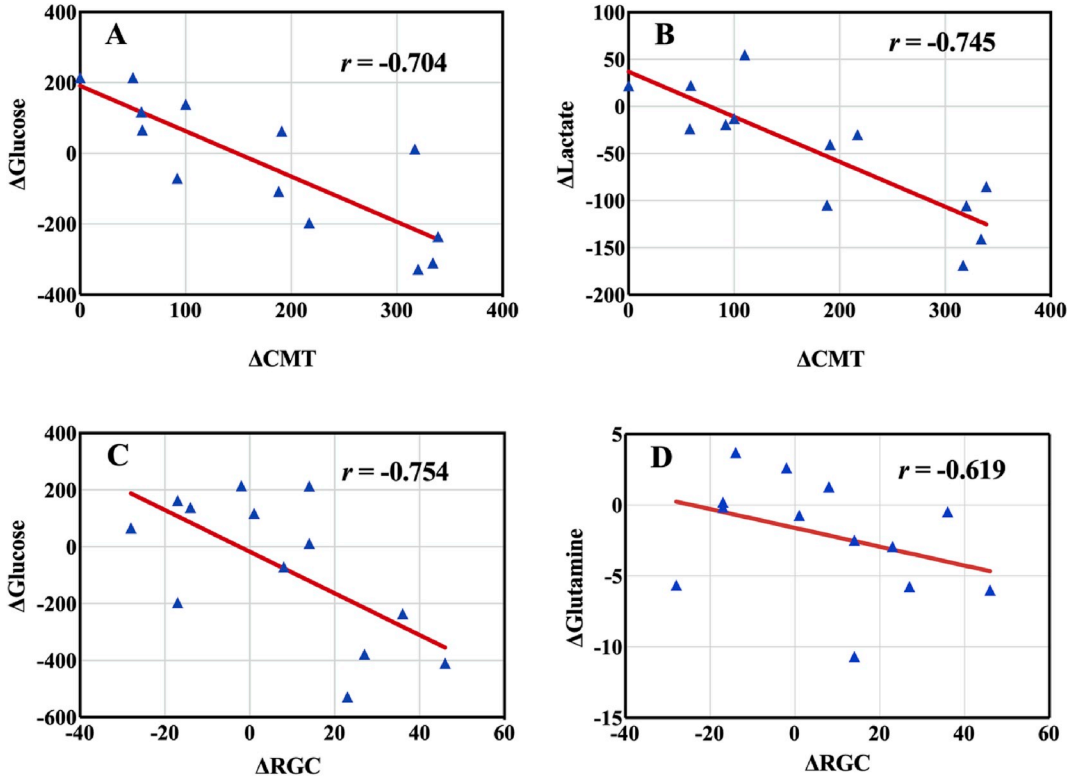

Fig. 4. The scatter plots demonstrated the negative correlation between the change of central macular thickness (ΔCMT) and aqueous metabolic changes in glucose (A) and lactate(B) in CRVO patients before and after intravitreal anti-VEGF injection; the scatter plots demonstrated the negative correlation between the change of retinal ganglion cell thickness(ΔGCL) and aqueous metabolic changes in glucose(C) and glutamine(D) in CRVO patients before and after intravitreal anti-VEGF injection; the solid line represents the regression line.

reductive is regarded as a major carbon source of fatty acid synthesis (Metallo et al., 2011; Mullen et al., 2011). Fendt and colleagues reported that a decreased K/C ratio promotes the reductive generation of citrate under hypoxic conditions (Fendt et al., 2013). Our data identified a higher K/C ratio for the AH of patients with cataracts (1.73 ± 0.51), compared to patients with CRVO (1.17 ± 0.10). Moreover, the K/C ratio had a strong positive correlation with glutamine in the CRVO group (Fig. 2C). However, without glutamine isotope-labeled, we could not confirm the correlation between K/C ratio and reductive carboxylation at the current stage. The close correlation between K/C ratio and glutamine might be associated with glutamine oxidation or synthesis. Overall, these results suggest that glutamine might have a critical role in CRVO pathogenesis.

Previous studies have suggested that diabetes is accompanied by an accumulation of glutamate in the retina, which leads to neurotoxicity and the development of diabetic retinopathy (Rhee et al., 2018), decreased glutamate levels in the retina during the first month of diabetes have also been reported (Vilchis and Salceda, 1996), which is consistent with our findings. Because the average duration of onset for patients included in this study was less than one month, further clinical evaluations with longer follow-up periods are required to investigate this relationship.

Interestingly, our data also showed an upward trend for lactate for patients with CRVO, although no statistically significant differences were detected. The Pasteur effect is also considered to be the compensatory mechanism for cells to resist mitochondrial impairment (Winkler et al., 2003). Thus, we estimated that the increased lactic acid level in AH reflects the aggravating hypoxia condition and adaptive mechanism via glycolysis pathway from CRVO eye tissues in human.

In addition to this result, we also observed a downward trend in succinate levels for the CRVO group (1.56 ± 0.37 μg/ml) compared to controls (4.10 ± 1.20 μg/ml). Several explanations might contribute to this. First possible explanation for the concurrent increase in lactate and the decrease in succinate observed in our CRVO group is mitochondrial damage. Secondly, succinate has the ability to increase glycolysis by driving hypoxia-inducible factor-1a (HIF-1a) accumulation (Mills and O'Neill, 2014). However, succinate has been reported to accumulate in the vitreous fluid of patients with proliferative diabetic retinopathy, but no increase was seen in the AH (Matsumoto et al., 2012). These differences are likely due to differences in oxygen demand and mitochondrial reserve capacity between the retina, ciliary body, and iris (Jin et al., 2019; Kooragayala et al., 2015). As such, we propose an alternative reason for the concurrent lactate increase and succinate decrease in our CRVO group: that the ciliary body and iris might compensate for perturbances in energy homeostasis and production of ROS by relying more heavily on glycolysis as an essential route for energy production. However, further research is needed to validate this speculation.

Surprisingly, no significant differences in the concentrations of other metabolites between the controls and CRVO group were detected in our study. This may be due to low rates of diffusion between the vitreous fluid into the AH for these substances or high turnover rates within the AH. With the vitreous fluid assuming a gel structure, movement and diffusion of substances into the AH is relatively slow (Wakabayashi et al., 2006). In addition, some metabolic changes associated with CRVO are only slight. Due to the limited sample size of this study, we were possibly unable to detect smaller metabolic alterations; therefore, future larger studies are warranted.

Intravitreal injections of anti-VEGF drugs are widely used to treat CRVO; however, outcomes are highly variable. Thus, for achieving better outcomes, it is essential to obtain a better understanding of the metabolic processes that follow anti-VEGF interventions. After anti-VEGF treatment, lactate levels were significantly elevated. It has been suggested that anti-VEGF treatment is associated with alleviating

macular edema in CRVO pathogenesis (Cehofski et al., 2017). Hence, increased lactate levels might be attributed to an increased demand on anaerobic glycolysis for macular energy production in retina tissues during recovery.

Despite its prevalent role in the treatment of RVO, a number of recent studies have also reported associations between long-term anti-VEGF treatment and the development of ganglion cell layer atrophy. Similarly, our data showed decreases in RGC thickness for patients with CRVO after anti-VEGF therapy. The RGC is sensitive to both acute and mild hypoxic stress and is possibly the first layer affected by RVO (Khayat et al., 2018; Lim et al., 2015). Both apoptotic and necrotic changes have been reported for ganglion cells in experimental models of CRVO. Interestingly, changes in RGC thickness observed in our study were negatively correlated with increases in glucose and glutamine (Fig. 4C and D). Because glutamine and glucose are both utilized as a carbon source for biosynthesis, these correlations may be indicative of a recovery response. However, the small sample size and poorly matched group sizes in our study meant that we had insufficient power to detect a statistically significant association.

5. Conclusions

In conclusion, these discoveries have expanded our understanding of the metabolic processes involved in CRVO. We report the first evidence that AH glucose metabolites are disturbed in CRVO. Our results indicate that glutamine was significantly decreased in the AH of CRVO and that perturbed glutamine metabolism is involved in CRVO pathogenesis. Furthermore, short-term anti-VEGF treatment alters glycolytic pathways involved in CRVO recovery responses. However, further investigation is necessary to confirm these findings.

Declaration of competing interest

The authors declare no conflicts of interest.

Acknowledgement

This work was supported by a grant from the National Natural Science Foundation of China (81700849) and Natural Science Foundation of Tianjin City (18JCQNJC10600).

Appendix A. Supplementary data

Supplementary data to this article can be found online at https://doi.org/10.1016/j.exer.2020.107919.

References

Barbas-Bernardos, C., Armitage, E.G., Garcia, A., Merida, S., Navea, A., Bosch-Morell, F., Barbas, C., 2016. Looking into aqueous humor through metabolomics spectacles - exploring its metabolic characteristics in relation to myopia. J. Pharm. Biomed. Anal. 127, 18–25.

Cehofski, L.J., Honore, B., Vorum, H., 2017. A review: proteomics in retinal artery occlusion, retinal vein occlusion, diabetic retinopathy and acquired macular disorders. Int. J. Mol. Sci. 18.

Drake, K.J., Sidorov, V.Y., McGuinness, O.P., Wasserman, D.H., Wikswo, J.P., 2012. Amino acids as metabolic substrates during cardiac ischemia. Exp. Biol. Med. 237, 1369–1378.

Du, J., Yanagida, A., Knight, K., Engel, A.L., Vo, A.H., Jankowski, C., Sadilek, M., Tran, V.T., Manson, M.A., Ramakrishnan, A., Hurley, J.B., Chao, J.R., 2016. Reductive carboxylation is a major metabolic pathway in the retinal pigment epithelium. Proc. Natl. Acad. Sci. U. S. A. 113, 14710–14715.

Eliasdottir, T.S., 2018. Retinal oximetry and systemic arterial oxygen levels. Acta Ophthalmol. 96 (Suppl. A113), 1–44.

Fendt, S.M., Bell, E.L., Keibler, M.A., Olenchock, B.A., Mayers, J.R., Wasylenko, T.M., Vokes, N.I., Guarente, L., Vander Heiden, M.G., Stephanopoulos, G., 2013. Reductive glutamine metabolism is a function of the alpha-ketoglutarate to citrate ratio in cells. Nat. Commun. 4, 2236.

Hu, R.G., Zhu, Y., Donaldson, P., Kalloniatis, M., 2012. Alterations of glutamate, glutamine, and related amino acids in the anterior eye secondary to ischaemia and reperfusion. Curr. Eye Res. 37, 633–643.

Hurley, J.B., Lindsay, K.J., Du, J., 2015. Glucose, lactate, and shuttling of metabolites in vertebrate retinas. J. Neurosci. Res. 93, 1079–1092.

Ishikawa, S., Nakazawa, M., Ishikawa, A., Ishiguro, S., Tamai, M., 1995. Alteration of glutamine concentration in the vitreous humor in patients with proliferative vitreoretinopathy. Curr. Eye Res. 14, 191–197.

Ji, Y., Rao, J., Rong, X., Lou, S., Zheng, Z., Lu, Y., 2017. Metabolic characterization of human aqueous humor in relation to high myopia. Exp. Eye Res. 159, 147–155.

Jin, H., Zhu, B., Liu, X., Jin, J., Zou, H., 2019. Metabolic characterization of diabetic retinopathy: an (1)H-NMR-based metabolomic approach using human aqueous humor. J. Pharm. Biomed. Anal. 174, 414–421.

Joyal, J.S., Gantner, M.L., Smith, L.E.H., 2018. Retinal energy demands control vascular supply of the retina in development and disease: the role of neuronal lipid and glucose metabolism. Prog. Retin. Eye Res. 64, 131–156.

Khayat, M., Williams, M., Lois, N., 2018. Ischemic retinal vein occlusion: characterizing the more severe spectrum of retinal vein occlusion. Surv. Ophthalmol. 63, 816–850.

Kooragayala, K., Gotoh, N., Cogliati, T., Nellissery, J., Kaden, T.R., French, S., Balaban, R., Li, W., Covian, R., Swaroop, A., 2015. Quantification of oxygen consumption in retina ex vivo demonstrates limited reserve capacity of photoreceptor mitochondria. Investig. Ophthalmol. Vis. Sci. 56, 8428–8436.

Lains, I., Gantner, M., Murinello, S., Lasky-Su, J.A., Miller, J.W., Friedlander, M., Husain, D., 2019. Metabolomics in the study of retinal health and disease. Prog. Retin. Eye Res. 69, 57–79.

Lim, H.B., Kim, M.S., Jo, Y.J., Kim, J.Y., 2015. Prediction of retinal ischemia in branch retinal vein occlusion: spectral-domain optical coherence tomography study. Investig. Ophthalmol. Vis. Sci. 56, 6622–6629.

Matsumoto, M., Suzuma, K., Maki, T., Kinoshita, H., Tsuiki, E., Fujikawa, A., Kitaoka, T., 2012. Succinate increases in the vitreous fluid of patients with active proliferative diabetic retinopathy. Am. J. Ophthalmol. 153, 896–902 e891.

Mayordomo-Febrer, A., Lopez-Murcia, M., Morales-Tatay, J.M., Monleon-Salvado, D., Pinazo-Duran, M.D., 2015. Metabolomics of the aqueous humor in the rat glaucoma model induced by a series of intracamerular sodium hyaluronate injection. Exp. Eye Res. 131, 84–92.

Metallo, C.M., Gameiro, P.A., Bell, E.L., Mattaini, K.R., Yang, J., Hiller, K., Jewell, C.M., Johnson, Z.R., Irvine, D.J., Guarente, L., Kelleher, J.K., Vander Heiden, M.G., Iliopoulos, O., Stephanopoulos, G., 2011. Reductive glutamine metabolism by IDH1 mediates lipogenesis under hypoxia. Nature 481, 380–384.

Mills, E., O'Neill, L.A., 2014. Succinate: a metabolic signal in inflammation. Trends Cell Biol. 24, 313–320.

Mullen, A.R., Wheaton, W.W., Jin, E.S., Chen, P.H., Sullivan, L.B., Cheng, T., Yang, Y., Linehan, W.M., Chandel, N.S., DeBerardinis, R.J., 2011. Reductive carboxylation supports growth in tumour cells with defective mitochondria. Nature 481, 385–388.

Rhee, S.Y., Jung, E.S., Park, H.M., Jeong, S.J., Kim, K., Chon, S., Yu, S.Y., Woo, J.T., Lee, C.H., 2018. Plasma glutamine and glutamic acid are potential biomarkers for predicting diabetic retinopathy. Metabolomics 14, 89.

Santos-Fandila, A., Zafra-Gomez, A., Barranco, A., Navalon, A., Rueda, R., Ramirez, M., 2013. Quantitative determination of neurotransmitters, metabolites and derivates in microdialysates by UHPLC-tandem mass spectrometry. Talanta 114, 79–89.

Snytnikova, O.A., Khlichkina, A.A., Yanshole, L.V., Yanshole, V.V., Iskakov, I.A., Egorova, E.V., Stepakov, D.A., Novoselov, V.P., Tsentalovich, Y.P., 2016. Metabolomics of the human aqueous humor. Metabolomics 13.

Song, P., Xu, Y., Zha, M., Zhang, Y., Rudan, I., 2019. Global epidemiology of retinal vein occlusion: a systematic review and meta-analysis of prevalence, incidence, and risk factors. J Glob Health 9 010427.

Tang, Z., Cao, T., Lin, S., Fu, L., Li, S., Guan, X.Y., Cai, Z., 2016. Characterization of oncogene-induced metabolic alterations in hepatic cells by using ultrahigh performance liquid chromatography-tandem mass spectrometry. Talanta 152, 119–126.

Trainor, P.J., Hill, B.G., Carlisle, S.M., Rouchka, E.C., Rai, S.N., Bhatnagar, A., DeFilippis, A.P., 2017. Systems characterization of differential plasma metabolome perturbations following thrombotic and non-thrombotic myocardial infarction. J Proteomics 160, 38–46.

Trivedi, D.K., Hollywood, K.A., Goodacre, R., 2017. Metabolomics for the masses: the future of metabolomics in a personalized world. New Horiz Transl Med 3, 294–305.

Vilchis, C., Salceda, R., 1996. Effect of diabetes on levels and uptake of putative amino acid neurotransmitters in rat retina and retinal pigment epithelium. Neurochem. Res. 21, 1167–1171.

Wakabayashi, Y., Yagihashi, T., Kezuka, J., Muramatsu, D., Usui, M., Iwasaki, T., 2006. Glutamate levels in aqueous humor of patients with retinal artery occlusion. Retina 26, 432–436.

Wang, H., Fang, J., Chen, F., Sun, Q., Xu, X., Lin, S.H., Liu, K., 2019. Metabolomic profile of diabetic retinopathy: a GC-TOFMS-based approach using vitreous and aqueous humor. Acta Diabetol. https://doi.org/10.1007/s00592-019-01363-0. In press.

Winkler, B.S., 1981. Glycolytic and oxidative metabolism in relation to retinal function. J. Gen. Physiol. 77, 667–692.

Winkler, B.S., Arnold, M.J., Brassell, M.A., Puro, D.G., 2000. Energy metabolism in human retinal Muller cells. Investig. Ophthalmol. Vis. Sci. 41, 3183–3190.

Winkler, B.S., Sauer, M.W., Starnes, C.A., 2003. Modulation of the Pasteur effect in retinal cells: implications for understanding compensatory metabolic mechanisms. Exp. Eye Res. 76, 715–723.

Winkler, B.S., Starnes, C.A., Sauer, M.W., Firouzgan, Z., Chen, S.C., 2004. Cultured retinal neuronal cells and Muller cells both show net production of lactate. Neurochem. Int. 45, 311–320.

Wu, G., 2009. Amino acids: metabolism, functions, and nutrition. Amino Acids 37, 1–17.

Yao, J., Chen, Z., Yang, Q., Liu, X., Chen, X., Zhuang, M., Liu, Q., 2013. Proteomic analysis of aqueous humor from patients with branch retinal vein occlusion-induced macular edema. Int. J. Mol. Med. 32, 1421–1434.

Young, S.P., Wallace, G.R., 2009. Metabolomic analysis of human disease and its application to the eye. J Ocul Biol Dis Infor 2, 235–242.

Yuan, M., Breitkopf, S.B., Yang, X., Asara, J.M., 2012. A positive/negative ion-switching, targeted mass spectrometry-based metabolomics platform for bodily fluids, cells, and fresh and fixed tissue. Nat. Protoc. 7, 872–881.